

Supplementary Information

1. Methods

1.1. Age estimation

Age can be estimated from FL using validated FL:age Von Bertalanffy growth curves for blue sharks (Natanson & Skomal 2003) and porbeagles (Natanson et al. 2002). The FL of sequential vertebral samples from individual sharks can be estimated from sample VR (distance of each sample from the vertebral centrum along VR) using VR:FL relationships.

Validated VR:FL relationships exist for blue shark (Natanson & Skomal 2003) and porbeagle (Natanson et al. 2002) trunk vertebrae, whereas a relationship for blue shark cervical vertebrae was estimated in this study from VR and FL data for cervical vertebrae from central and eastern blue sharks, constrained by VR and FL values at birth estimated from age at birth = 0 years using inverse validated FL:age and VR:FL relationships for blue shark trunk vertebrae (Fig. S1).

Nevertheless, VR and FL data for trunk vertebrae from sharks examined here were somewhat offset from the validated relationships, most likely due to errors or approximations in the measured VR or because vertebrae were excised from an even slightly different position along the spinal cord. Clearly, smaller (or potentially greater) measured VR compared to the VR that would be predicted at a FL by the VR:FL relationship, would result in under (over) prediction of FL, which would then propagate exponentially to age estimates.

To account for this issue and improve comparability of age estimates across individuals, we calculated an adjusted VR from FL data for each shark using inverse validated VR:FL relationships for trunk vertebrae from porbeagles and western blue sharks, and the inverse estimated relationship for cervical vertebrae from central and eastern blue sharks. This correction assumes that VR:FL relationships are exact, but corrects for difference between the measured VR and the VR that would be predicted at a FL by VR:FL relationships, and thus for under (over) prediction of FL and age from measured VR.

When age was estimated for sequential samples collected along VR, the adjusted VR was used to calculate the (achieved) average interval between adjacent samples (*AvgInt*, mm) for each vertebra (Eqn. S1).

$$AvgInt = \frac{AdjVR}{N} \quad (S1)$$

where *AdjVR* (mm) is the adjusted VR, *N* is the number of sequential samples collected for the vertebra.

The median distance along (adjusted) VR (*d*, mm) was calculated for each sample (Eqn. S2).

$$d = SampleID \cdot AvgInt - \frac{AvgInt}{2} \quad (S2)$$

where *sampleID* is the sequential number of each sample along VR. In time-series analysis, where combined samples are displayed as duplicated datapoints with different age but same isotope values, sample distance along VR was calculated for each sample in the combination and *sampleID* was therefore the ID of each single sample in the combination. In variance analysis, where combined samples are single datapoints with age calculated for the combined sample and isotope

values measured in the combined sample, sampleID was the mean of IDs of samples in the combination: e.g., if samples 1+2 were combined, sampleID = 1.5.

Sample distance was converted to FL using the validated VR:FL relationships for blue shark and porbeagle trunk vertebrae (Eqns. S3-S4) and the estimated relationship for blue shark cervical vertebrae (Eqn. S5).

$$\log(FL) = a \cdot \log(d) + b \quad (S3)$$

which, solving for FL, becomes

$$FL = e^{a \cdot \log(d) + b} \quad (S4)$$

$$FL = a_{bsh-cerv} \cdot d + b_{bsh-cerv} \quad (S5)$$

$a = 0.89$ and $b = 3.10$ for blue shark (combined sexes) trunk vertebrae (Skomal & Natanson 2003), $a = 0.88$ and $b = 2.96$ for porbeagle (combined sexes) vertebrae (Natanson et al. 2002). In Eqn. S5, $a_{bsh-cerv} = 22.04$ and $b_{bsh-cerv} = -6.31$ (this study). These are coefficients for the linear VR:FL relationship estimated for blue shark cervical vertebrae using VR and FL data for cervical vertebrae from central and eastern blue sharks, constrained by VR and FL values at birth (estimated from age at birth = 0 years, using inverse validated FL:age and VR:FL relationships for trunk vertebrae).

Sample estimated FL was then converted to age using validated FL:age Von Bertalanffy growth curves for blue sharks and porbeagles (Eqn. S6).

$$age = \frac{\log(1 - \frac{FL}{FL_{max}})}{-K} + age_0 \quad (S6)$$

For blue sharks, $FL_{max} = 310.00$, $K = 0.13$ and $age_0 = -1.77$ (females; Skomal & Natanson 2003); for porbeagles, $FL_{max} = 289.40$, $K = 0.07$ and $age_0 = -6.06$ (combined sexes; Natanson et al. 2002).

Note that the curve is steeper and reaches the plateau phase more quickly in blue sharks, accounting for difference in longevity between the two species. Also, FL values at birth calculated from age at birth = 0 years using inverse validated FL:age relationships were 64 and 100 cm for blue sharks and porbeagles, respectively. These values were greater than previously reported mean measured FL values at birth (45 and 67 for blue sharks and porbeagles, respectively). This meant that, for mean measured FL values at birth, validated Von Bertalanffy growth curves predicted negative ages of -0.6 years in blue sharks and -2.3 years in porbeagles. For porbeagles in particular, small FL values estimated for samples collected near the core of vertebral sections corresponded to negative ages up to -6 years, due to the reduced steepness of validated Von Bertalanffy growth curve by Natanson et al. 2002 compared to as if this relationship was constrained by a FL value at birth of 67 cm (rather than 100 cm) at age at birth = 0 years. This means that Von Bertalanffy growth curves are not applicable to estimate age during the pre-birth stage, therefore sample age is not displayed in plots for pre-birth samples.

2. Results

2.1. Individual profiles

2.1.1. Bulk protein

Within-individual variability in ontogenetic profiles of raw $\delta^{13}\text{C}$ and $\delta^{15}\text{N}$ values reflected a long-term ontogenetic pattern overlain by short-term excursions in all blue sharks and porbeagles except individual 11 in all blue sharks and porbeagles except the porbeagle 11 (Fig. S4). Profiles of raw $\delta^{13}\text{C}$ and $\delta^{15}\text{N}$ values were highly variable among individuals. Profiles of $\delta^{13}\text{C}$ values were consistent across the three blue sharks from the Northwest Atlantic, with $\delta^{13}\text{C}$ values decreasing around birth and increasing back to pre-birth levels during juvenile and early adult growth (Fig. S4G-I). Profiles were more variable in central and eastern North Atlantic blue sharks: $\delta^{13}\text{C}$ values increased linearly through ontogeny with a few small excursions in individuals 12 and 131, linearly with regular pronounced oscillations in sharks 16 and 101, and with a U-shape in individuals 24 and 33 (except for a pronounced excursion in the juvenile stage in individual 33; Fig. S4A-F). This U-shape resembles the pattern shown by Northwest Atlantic individuals. No evident consistencies were observed in profiles of $\delta^{15}\text{N}$ values across areas or individuals (Fig. S4A-I).

Profiles of $\delta^{13}\text{C}$ values were similar across the three porbeagles from the Northwest Atlantic and more variable among individuals from the Northeast Atlantic (Fig. S4J-O). In the former group, $\delta^{13}\text{C}$ values remained relatively constant through ontogeny, with a pronounced negative excursion around birth and moderate excursions in juvenile and subadult stages (Fig. S4M-O). In individuals from the Northeast Atlantic, values of $\delta^{13}\text{C}$ decreased just before birth and increased back to maternal levels in juvenile and subadult stages in individual 11, increased slightly with regular excursions in individual 40, and increased in late pre-birth and early juvenile stages and decreased in juvenile and subadult stages in individual 1000 (Fig. S4J-L). Values of $\delta^{15}\text{N}$ increased stepwise at an age of ~8-13 years and reached a plateau at an age of ~13 years in Northwest Atlantic porbeagles (Fig. S4M-O). No similar increase was observed in subadult porbeagles from the Northeast Atlantic. Values of $\delta^{15}\text{N}$ remained relatively constant throughout life in individuals 11 and 1000 and increased slightly with regular oscillations in individual 40 (Fig. S4J-L).

2.1.2. Essential amino acids

Similar to ontogenetic profiles in $\delta^{13}\text{C}$ values of bulk protein, within-individual variability in profiles of raw $\delta^{13}\text{C}_{\text{EAA}}$ and PC1_{EAA} values was given by a long-term (ontogenetic) pattern with superimposed short-term excursions (Fig. S5-S13 & S15). Profiles were highly variable, but commonalities and differences in profiles of PC1_{EAA} scores were observed among areas and individuals (Fig. S15). In blue sharks, PC1_{EAA} (hence $\delta^{13}\text{C}_{\text{EAA}}$) values increased throughout life in all sharks but individual 33, recovering patterns in bulk protein $\delta^{13}\text{C}$ values, despite patterns in PC1_{EAA} were dampened with respect to bulk $\delta^{13}\text{C}$ (Fig. S15A-I). Scores of PC1_{EAA} decreased sharply around birth and increased back to pre-birth levels prior to capture in all but 441 and 33 individuals. Short-term excursions in PC1_{EAA} were generally related to those in bulk $\delta^{13}\text{C}$ and more pronounced and frequent in individuals 335 and 441.

In porbeagles, PC1_{EAA} scores decreased slightly throughout life in individuals from the Northeast Atlantic and individual 599 and remained relatively constant in individuals 601 and 578 (Fig. S15J-O). This pattern is opposite to that observed in bulk protein $\delta^{13}\text{C}$ values. Scores of PC1_{EAA} decreased around birth in all sharks but individual 11. Excursions in PC1_{EAA} were related to those

in bulk protein $\delta^{13}\text{C}$ in individuals from the Northwest Atlantic (particularly the excursions around birth) but mostly independent in sharks from the Northeast Atlantic.

3. References

Kim, S. L., Tinker, M. T., Estes, J. A., and Koch, P. L. (2012). Ontogenetic and among-individual variation in foraging strategies of North East Pacific white sharks based on stable isotope analysis. *Plos One* 7, e45068.

Natanson, L. J., Mello, J. J., and Campana, S. E. (2002). Validated age and growth of the porbeagle shark, *Lamna nasus*, in the western North Atlantic Ocean. *Collective Volume of Scientific Papers ICCAT* 54, 1261-1279.

Newsome, S. D., Martinez del Rio, C., Bearhop, S., and Phillips, D. L. (2007). A niche for isotopic ecology. *Frontiers in Ecology and the Environment* 5, 429-436.

Skomal, G. B., and Natanson, L. J. (2003). Age and growth of the blue shark (*Prionace glauca*) in the North Atlantic Ocean. *Fishery Bulletin* 101, 627-639.

Figures

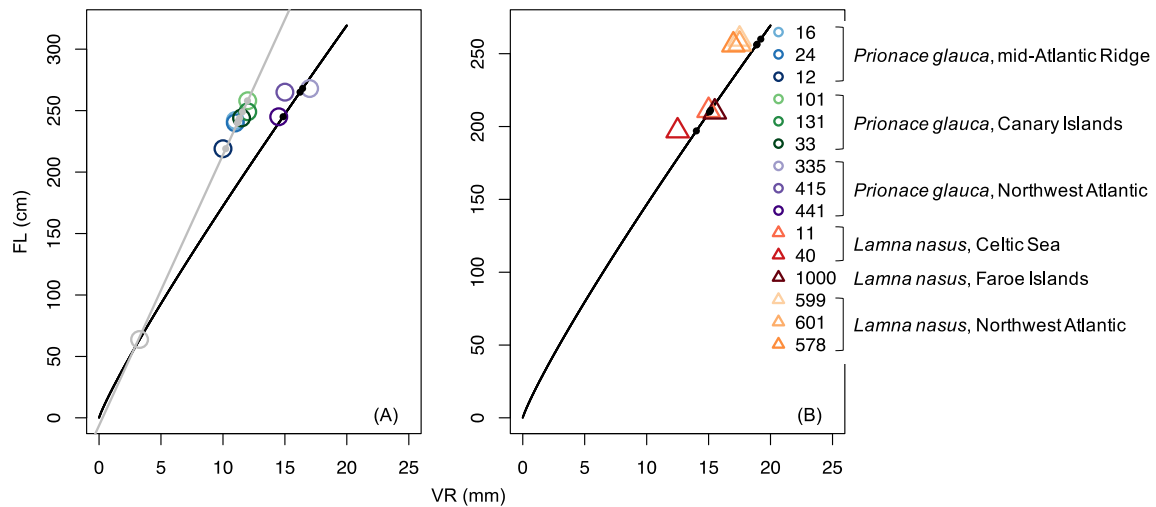


Figure S1. Validated VR:FL relationships for blue shark (*Prionace glauca*; A) and porbeagle (*Lamna nasus*; B) trunk vertebrae (black lines) and estimated relationship for blue shark cervical vertebrae from VR and FL data for cervical vertebrae from central and eastern blue sharks examined here, constrained by VR and FL values at birth (grey line). Measured VR and FL data are displayed for individual sharks (as in figure legend). Adjusted VR values were estimated from FL data using inverse VR:FL relationships to correct for errors or approximations in the measured VR, which would result in under (or over) prediction of FL and propagate exponentially to age. Adjusted VR values calculated with validated and estimated relationships and FL data are displayed as black and grey circles, respectively.

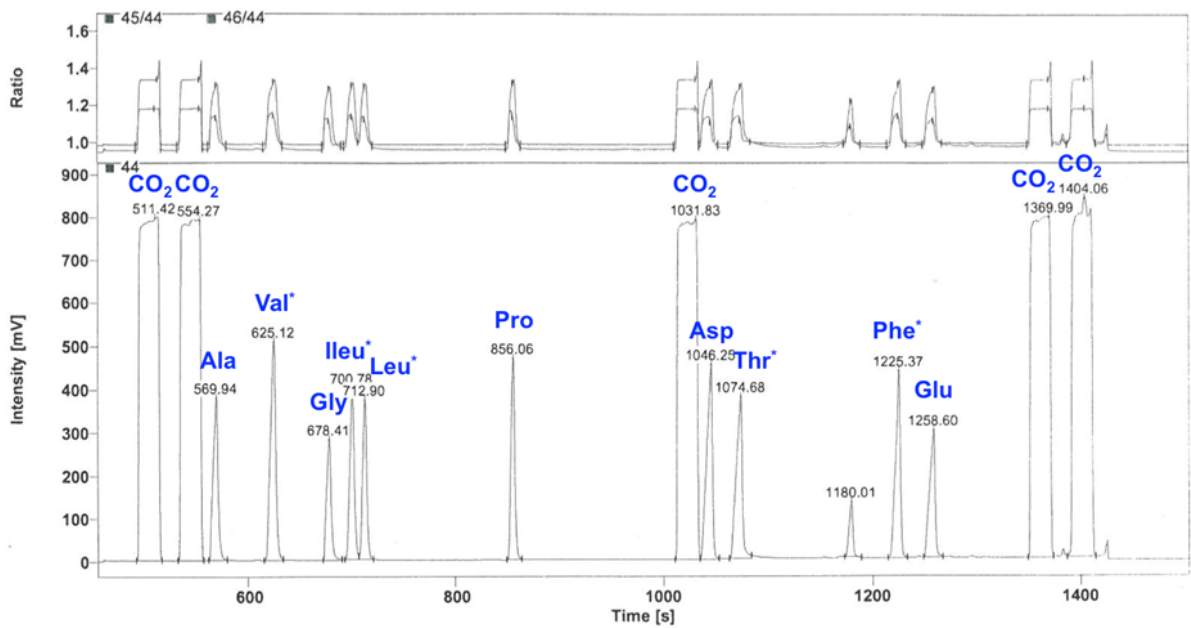


Figure S2. Typical chromatograph from the analysis of carbon isotope ratios in single amino acids. Peaks are labelled to indicate CO₂ reference and amino acids. Numbers indicate retention times. The peak with retention time = 1180.01 s is neither a CO₂ reference nor an amino acid peak, therefore is unresolved.

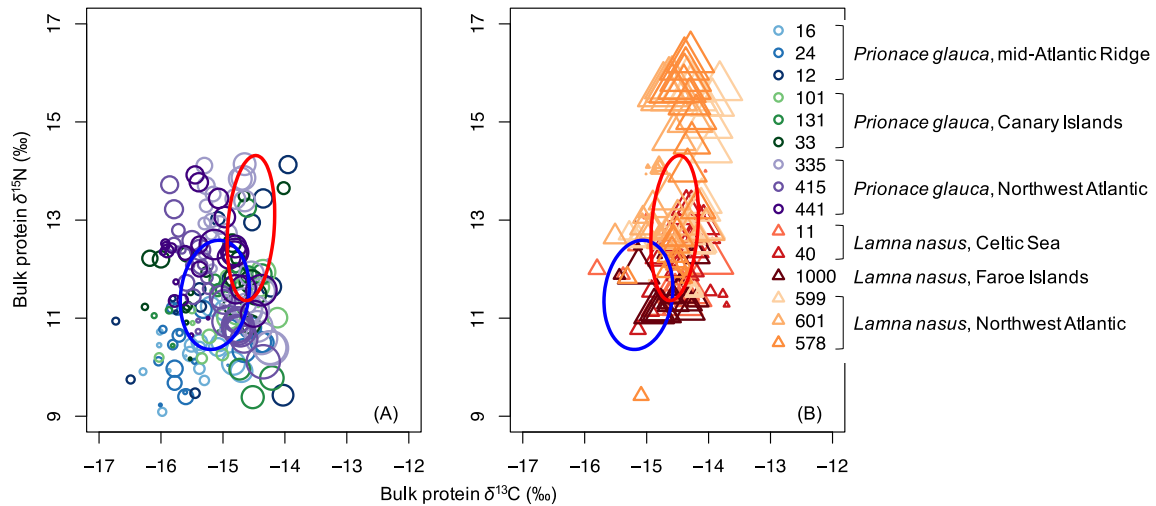


Figure S3. Biplot of bulk protein $\delta^{13}\text{C}$ versus $\delta^{15}\text{N}$ values in sequential vertebral samples from individual blue sharks and porbeagles caught across the North Atlantic (as in figure legend). Symbol size is proportional to sample distance along the vertebral radius. Ellipses represent standard ellipse areas corrected for small sample size (SEAc; Kim et al. 2012; Newsome et al. 2007); the blue ellipse is determined for blue sharks (1.93‰^2), the red ellipse for porbeagles (1.75‰^2). For clarity, blue shark and porbeagle samples are displayed in (A) and (B), respectively, along with the standard ellipse for the other species. The overlap for SEAc between blue sharks and porbeagles is 0.26‰^2 . The posterior probability that Bayesian-estimated standard ellipse area (SEA.B, $n = 20,000$) is larger for blue sharks than for porbeagles was 82%.

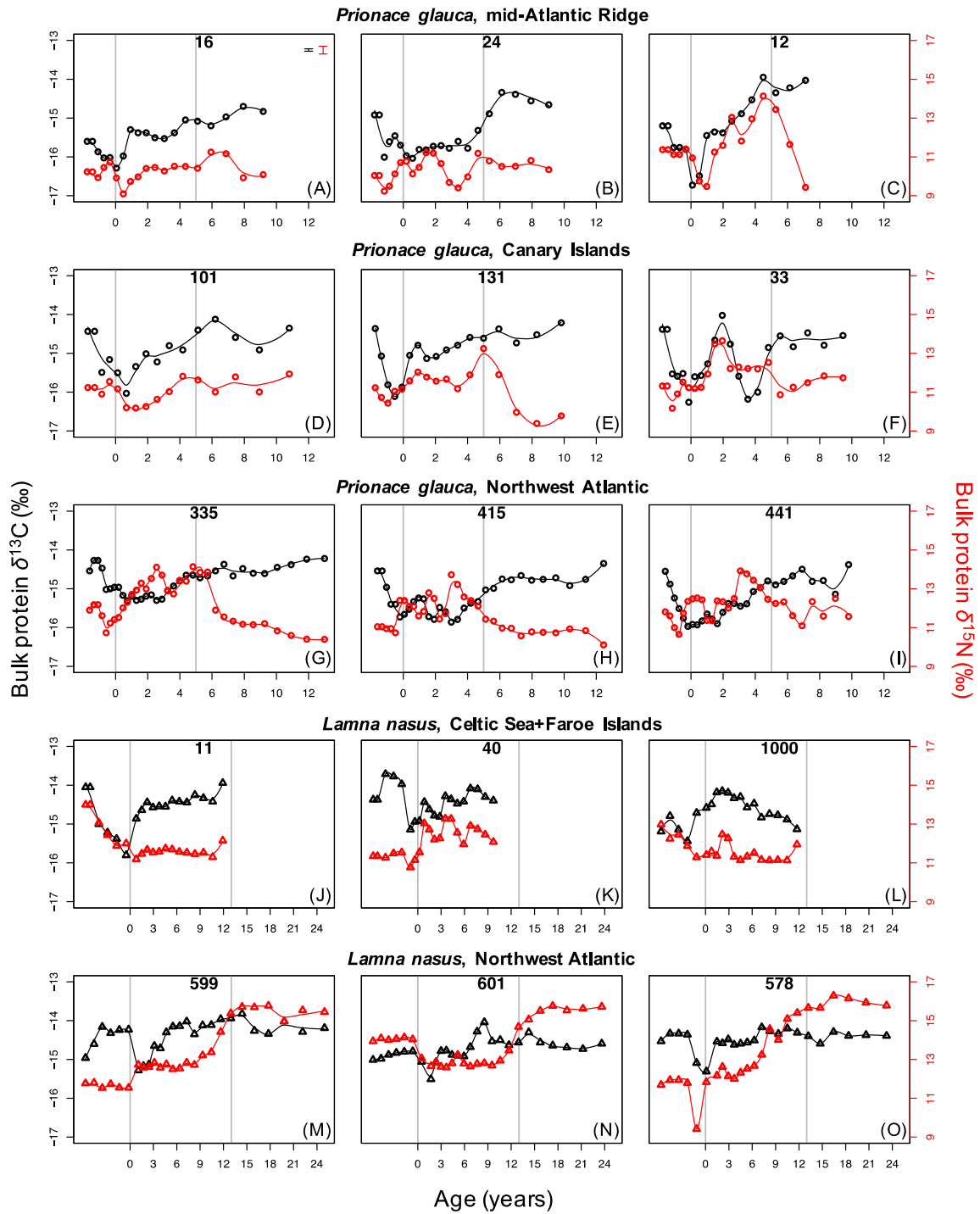


Figure S4. Individual profiles of $\delta^{13}\text{C}$ (black) and $\delta^{15}\text{N}$ (red) values of bulk protein in blue sharks from the mid-Atlantic Ridge (A-C), Canary Islands (D-F) and Northwest Atlantic (G-I), and porbeagles from the Celtic Sea (J-K) and Faroe Islands (L) and Northwest Atlantic (M-O). Individual ID is displayed at the top of each panel. Datapoints are measured values, lines are predicted values obtained by fitting the least smooth as possible Loess smoother. Grey vertical lines represent age at birth and at maturity and separate pre-birth, juvenile and adult life-history stages. Sample ages are not plotted in the pre-birth stage as Von Bertalanffy growth curves are not applicable to back-calculated age during this stage. The error bars in panel A are long-term standard deviations for $\delta^{13}\text{C}$ and $\delta^{15}\text{N}$ analyses.

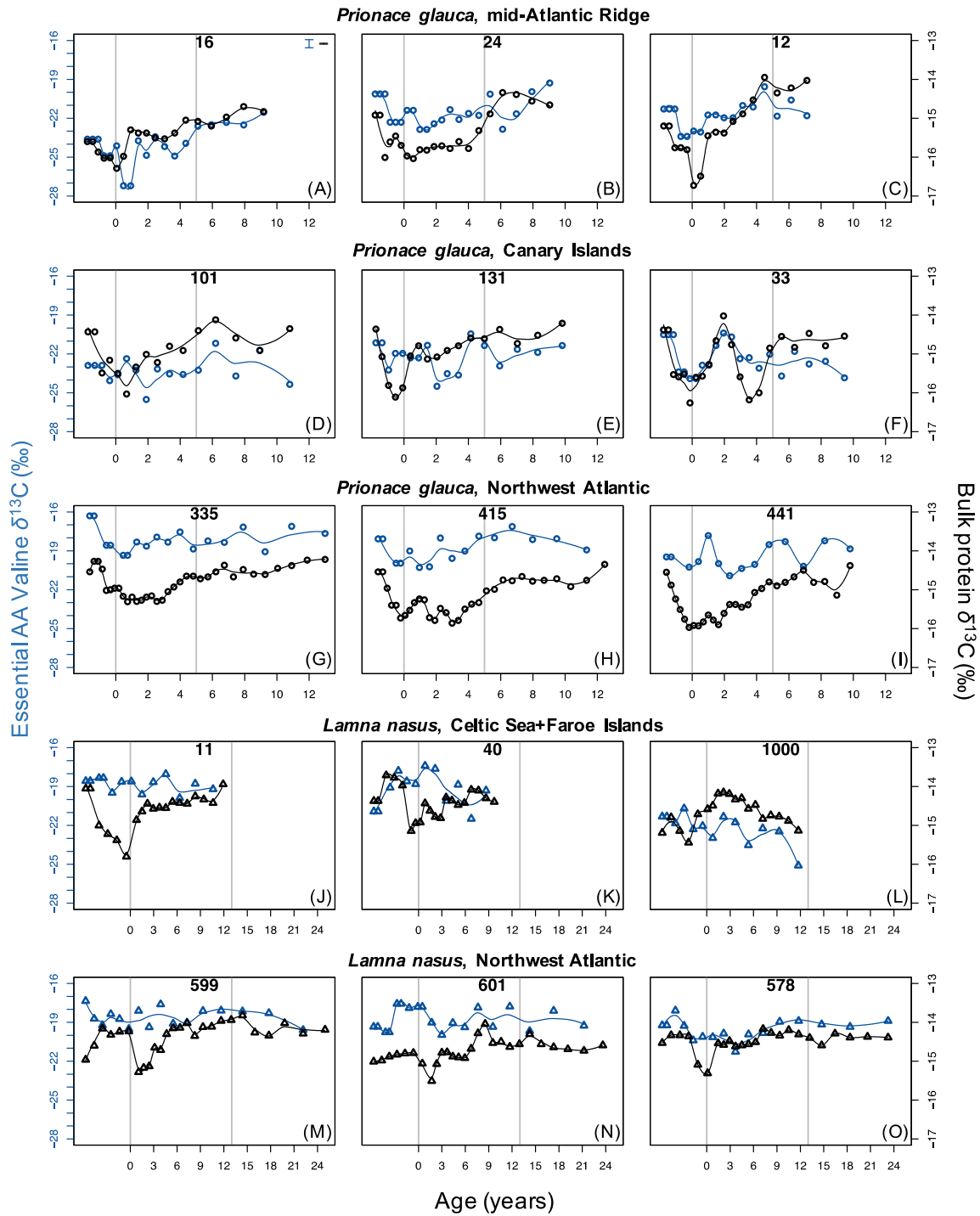


Figure S5. Individual profiles of $\delta^{13}\text{C}$ values of the essential amino acid valine (blue) and bulk protein (black). Figure description is the same as for Fig. S4. The error bars in panel A are long-term standard deviations for valine and bulk protein $\delta^{13}\text{C}$ analyses.

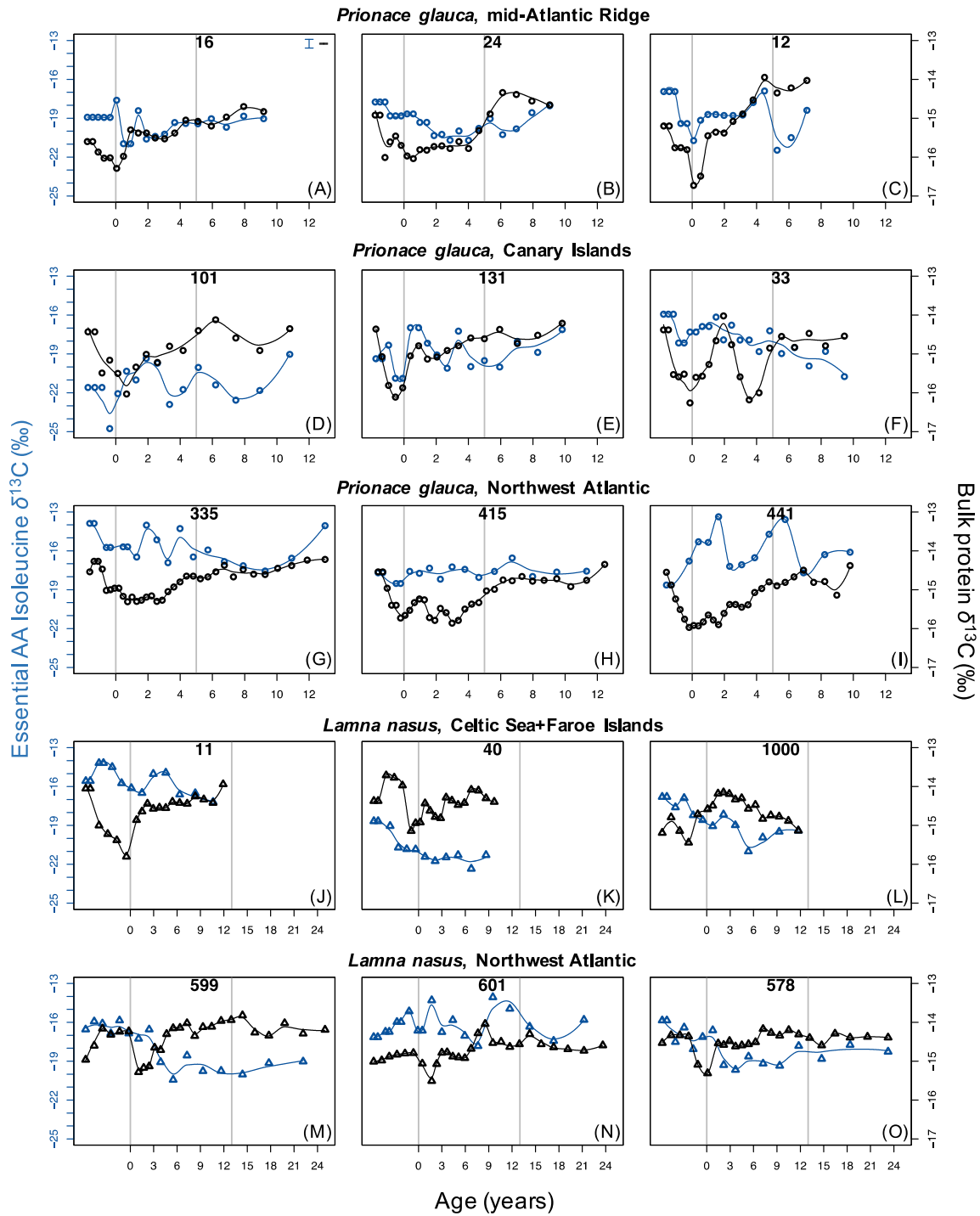


Figure S6. Individual profiles of $\delta^{13}\text{C}$ values of the essential amino acid isoleucine (blue) and bulk protein (black). Figure description is the same as for Fig. S4. The error bars in panel A are long-term standard deviations for isoleucine and bulk protein $\delta^{13}\text{C}$ analyses.

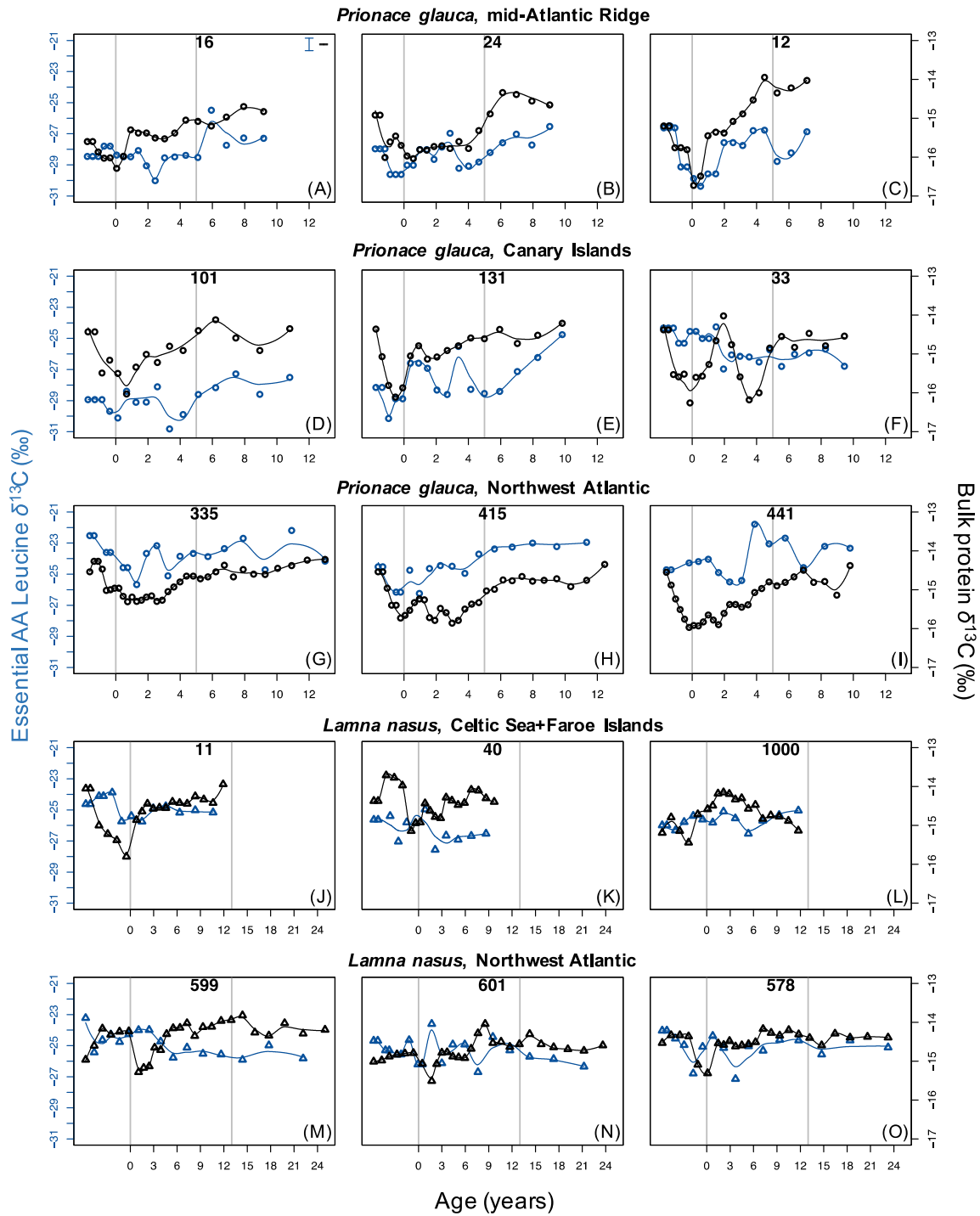


Figure S7. Individual profiles of $\delta^{13}\text{C}$ values of the essential amino acid leucine (blue) and bulk protein (black). Figure description is the same as for Fig. S4. The error bars in panel A are long-term standard deviations for leucine and bulk protein $\delta^{13}\text{C}$ analyses.

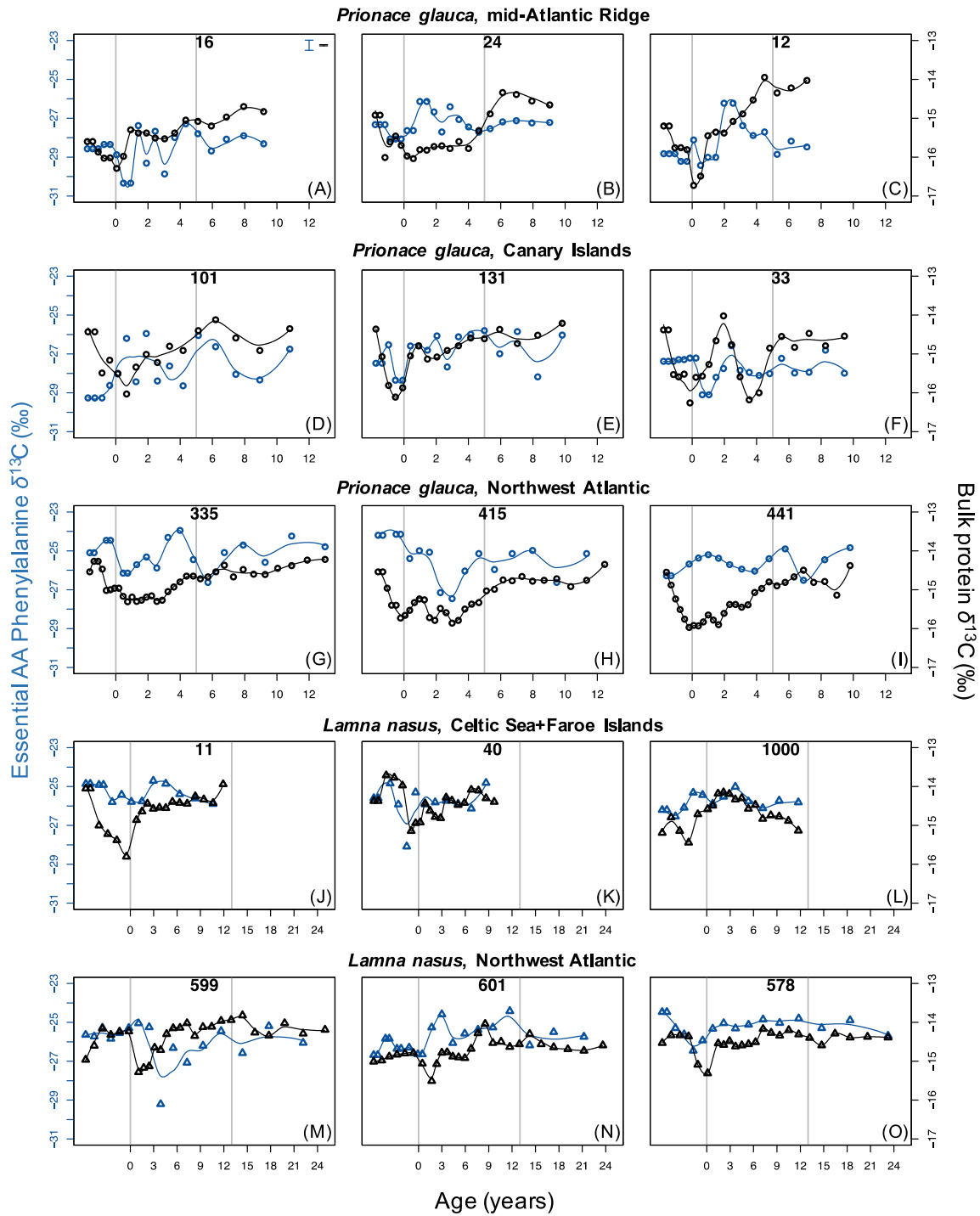


Figure S8. Individual profiles of $\delta^{13}\text{C}$ values of the essential amino acid phenylalanine (blue) and bulk protein (black). Figure description is the same as for Fig. S4. The error bars in panel A are long-term standard deviations for phenylalanine and bulk protein $\delta^{13}\text{C}$ analyses.

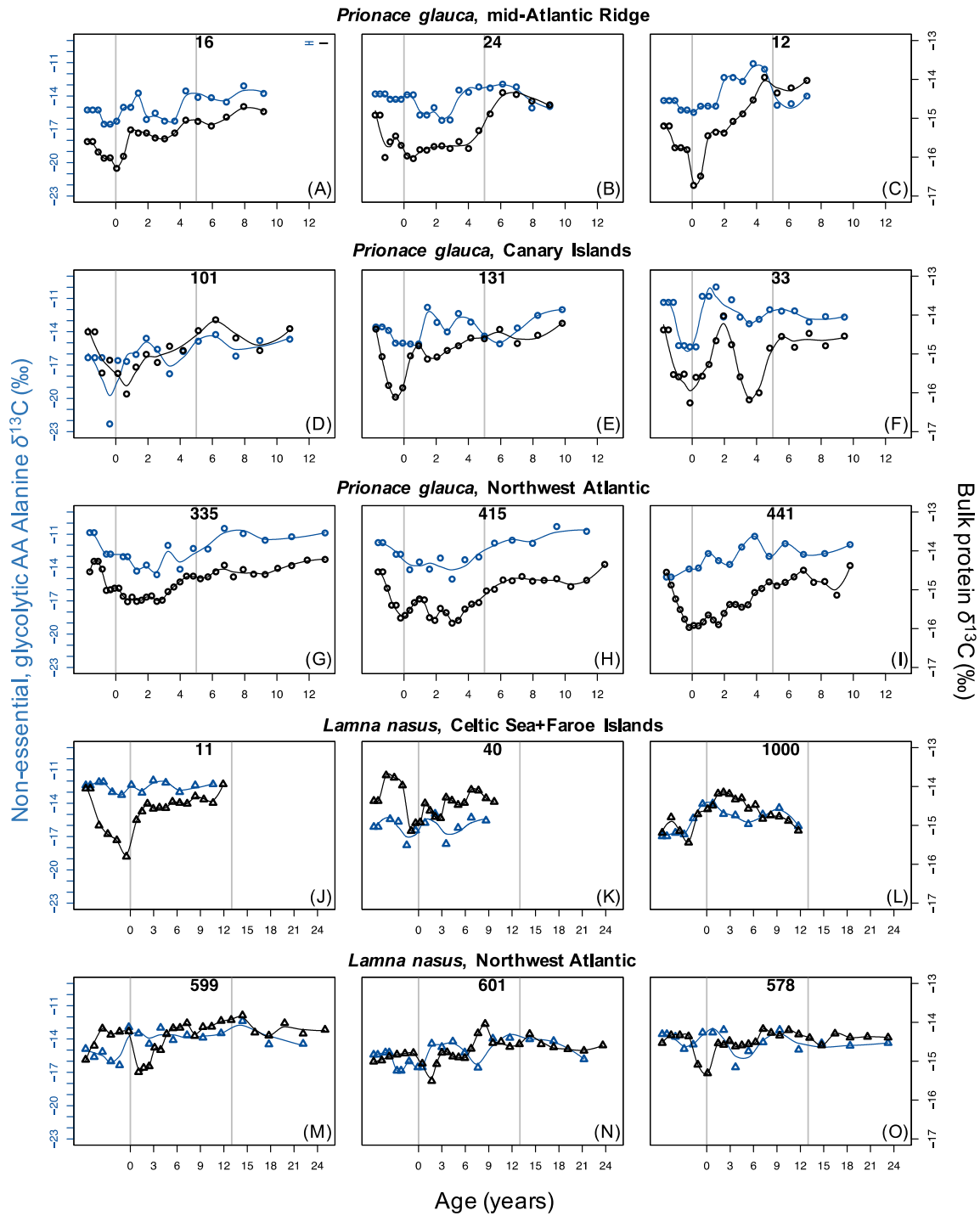


Figure S9. Individual profiles of $\delta^{13}\text{C}$ values of the non-essential, glycolytic amino acid alanine (blue) and bulk protein (black). Figure description is the same as for Fig. S4. The error bars in panel A are long-term standard deviations for alanine and bulk protein $\delta^{13}\text{C}$ analyses.

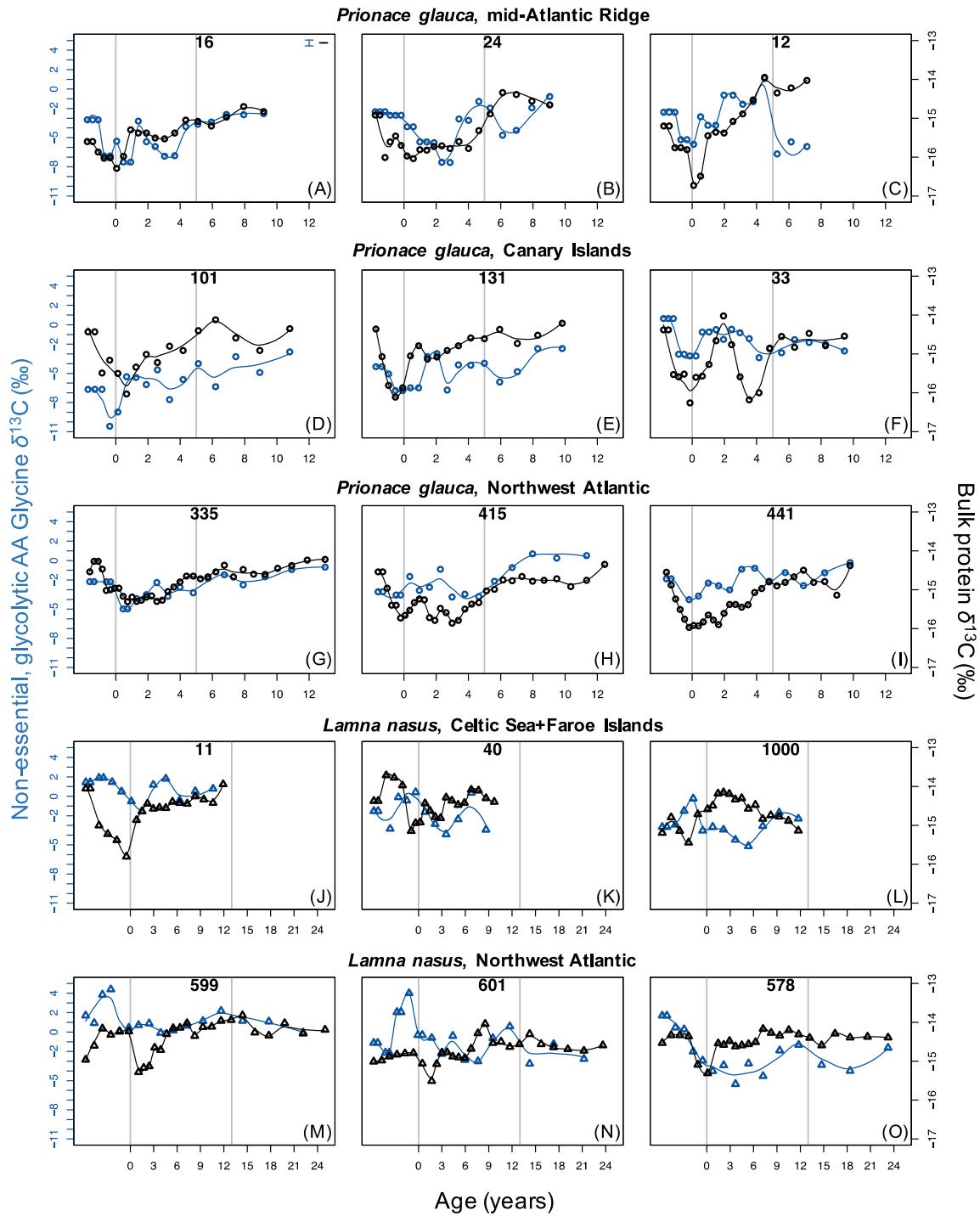


Figure S10. Individual profiles of $\delta^{13}\text{C}$ values of the non-essential, glycolytic amino acid glycine (blue) and bulk protein (black). Figure description is the same as for Fig. S4. The error bars in panel A are long-term standard deviations for glycine and bulk protein $\delta^{13}\text{C}$ analyses.

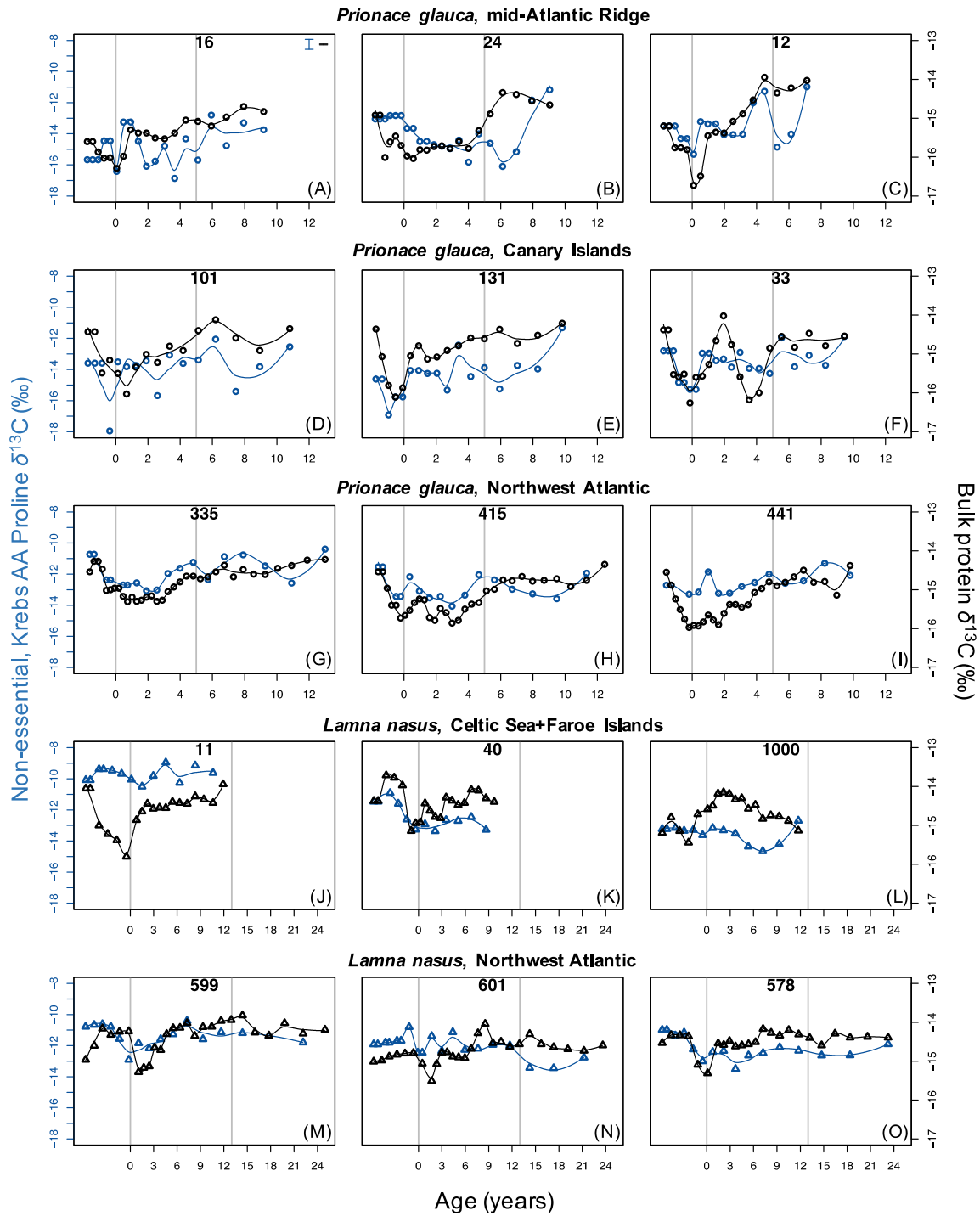


Figure S11. Individual profiles of $\delta^{13}\text{C}$ values of the non-essential, Krebs cycle amino acid proline (blue) and bulk protein (black). Figure description is the same as for Fig. S4. The error bars in panel A are long-term standard deviations for proline and bulk protein $\delta^{13}\text{C}$ analyses.

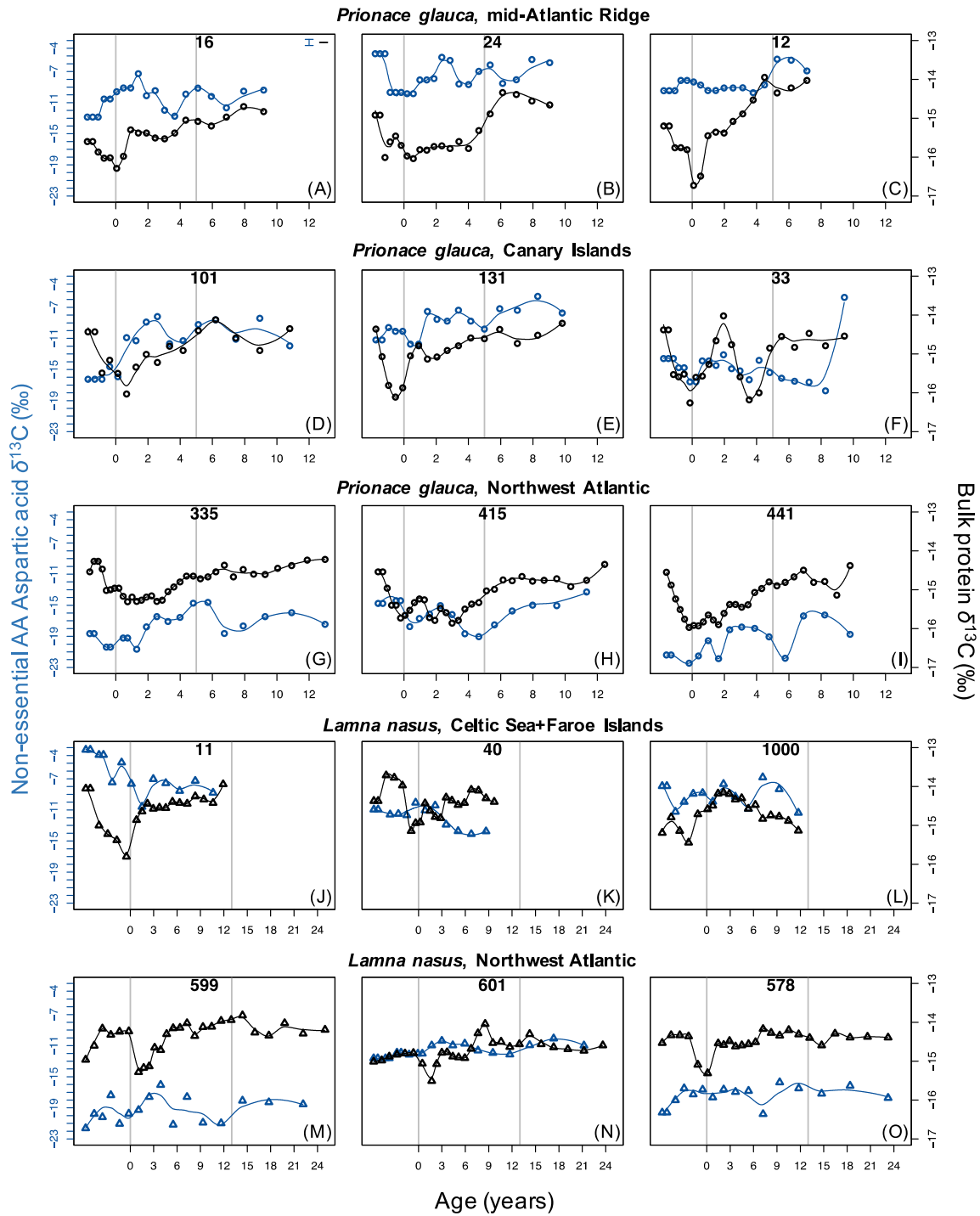


Figure S12. Individual profiles of $\delta^{13}\text{C}$ values of the non-essential amino acid aspartic acid (blue) and bulk protein (black). Figure description is the same as for Fig. S4. The error bars in panel A are long-term standard deviations for aspartic acid and bulk protein $\delta^{13}\text{C}$ analyses.

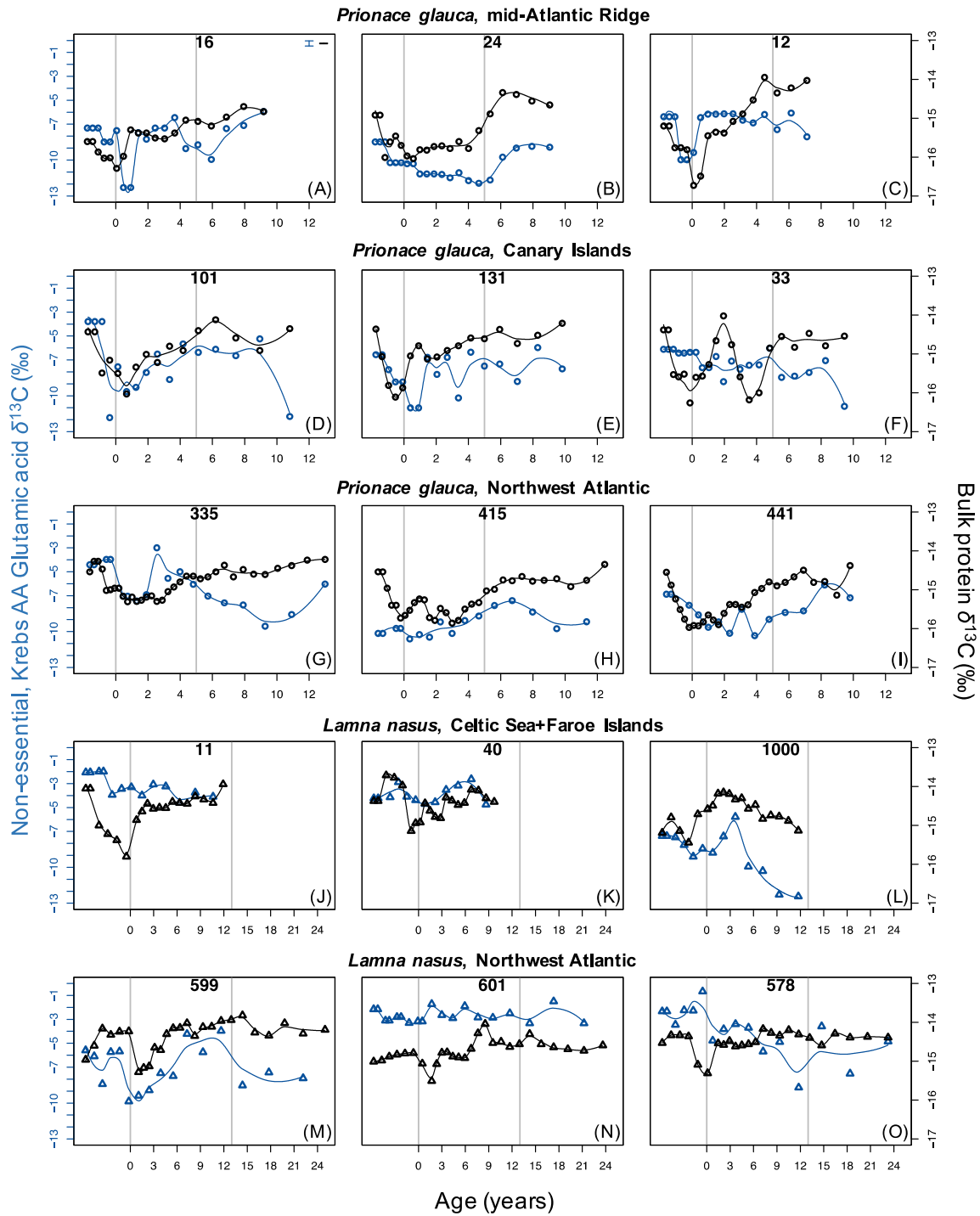


Figure S13. Individual profiles of $\delta^{13}\text{C}$ values of the non-essential, Krebs cycle amino acid glutamic acid (blue) and bulk protein (black). Figure description is the same as for Fig. S4. The error bars in panel A are long-term standard deviations for glutamic acid and bulk protein $\delta^{13}\text{C}$ analyses.

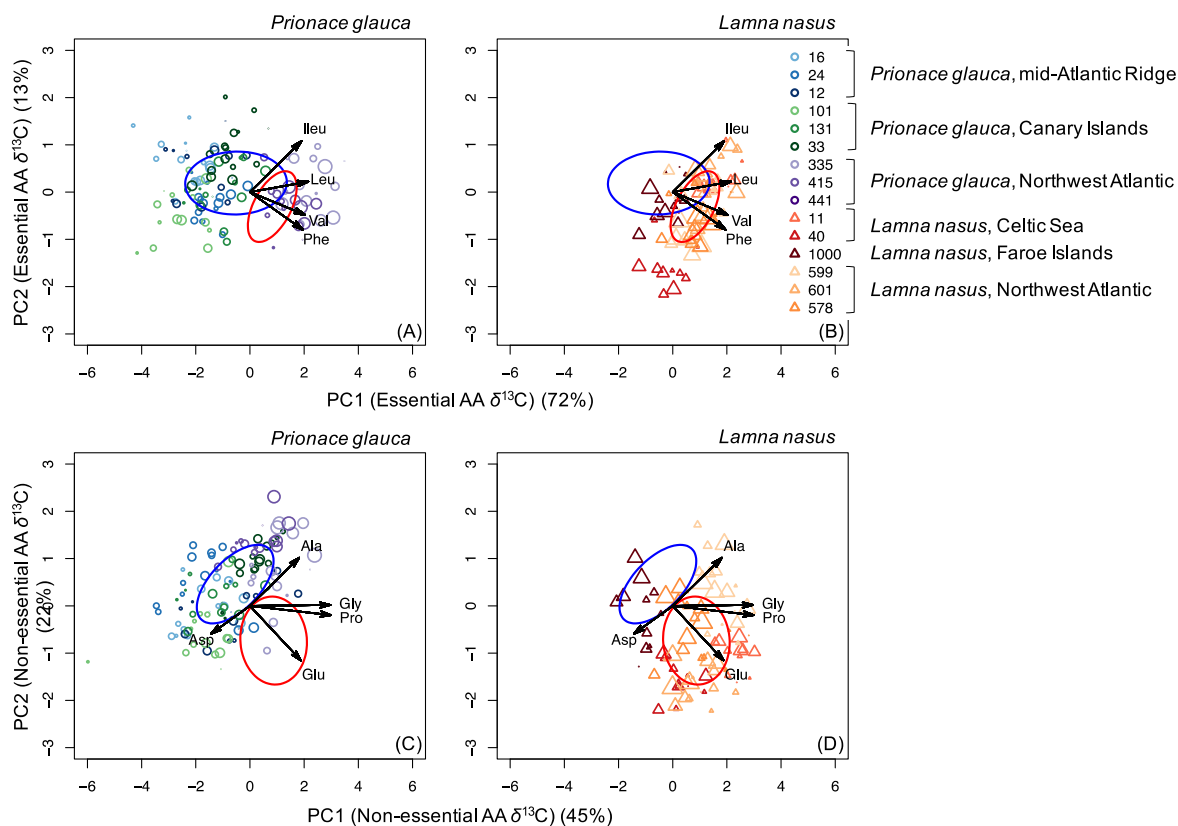


Figure S14. Principal component analysis (PCA) with $\delta^{13}\text{C}$ values of essential (Val = valine, Ileu = isoleucine, Leu = leucine and Phe = phenylalanine; A) and non-essential (Ala = alanine, Gly = glycine, Pro = proline, Asp = aspartic acid and Glu = glutamic acid; B) amino acids in sequential vertebral samples from individual blue sharks and porbeagles caught across the North Atlantic (as in figure legend). Symbol size is proportional to sample distance along the vertebral radius. Ellipses represent standard ellipse areas corrected for small sample size (SEAc); the blue ellipse is determined for blue shark, the red ellipse for porbeagles. For clarity, blue shark and porbeagle samples are displayed in (A) and (C) and (B) and (D), respectively, along with the standard ellipse for the other species.

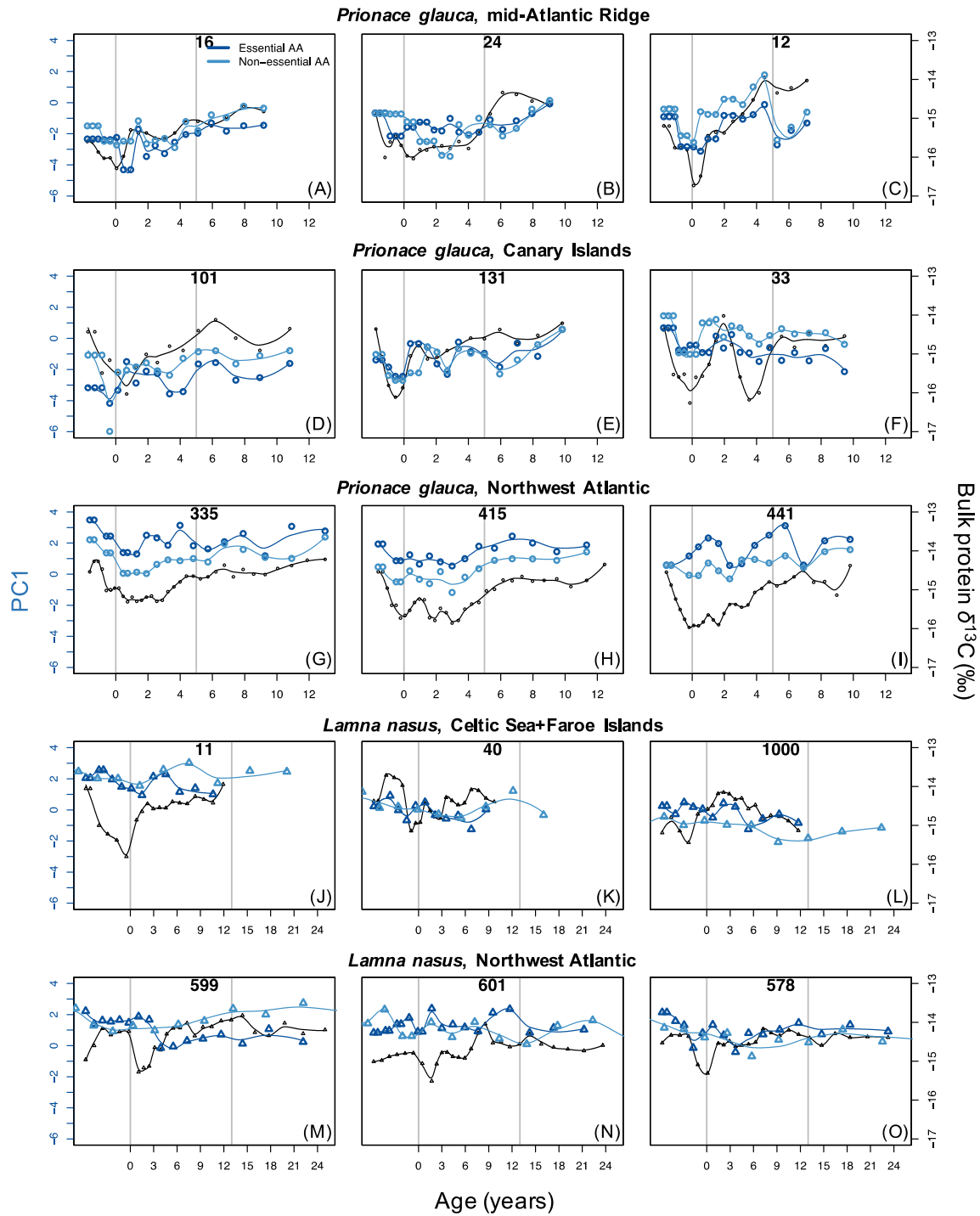


Figure S15. Individual profiles of PC1 values from PCAs with $\delta^{13}\text{C}$ values of essential amino acids (dark blue) and non-essential amino acids (light blue) and $\delta^{13}\text{C}$ values of bulk protein (black). Figure description is the same as for Fig. S4.

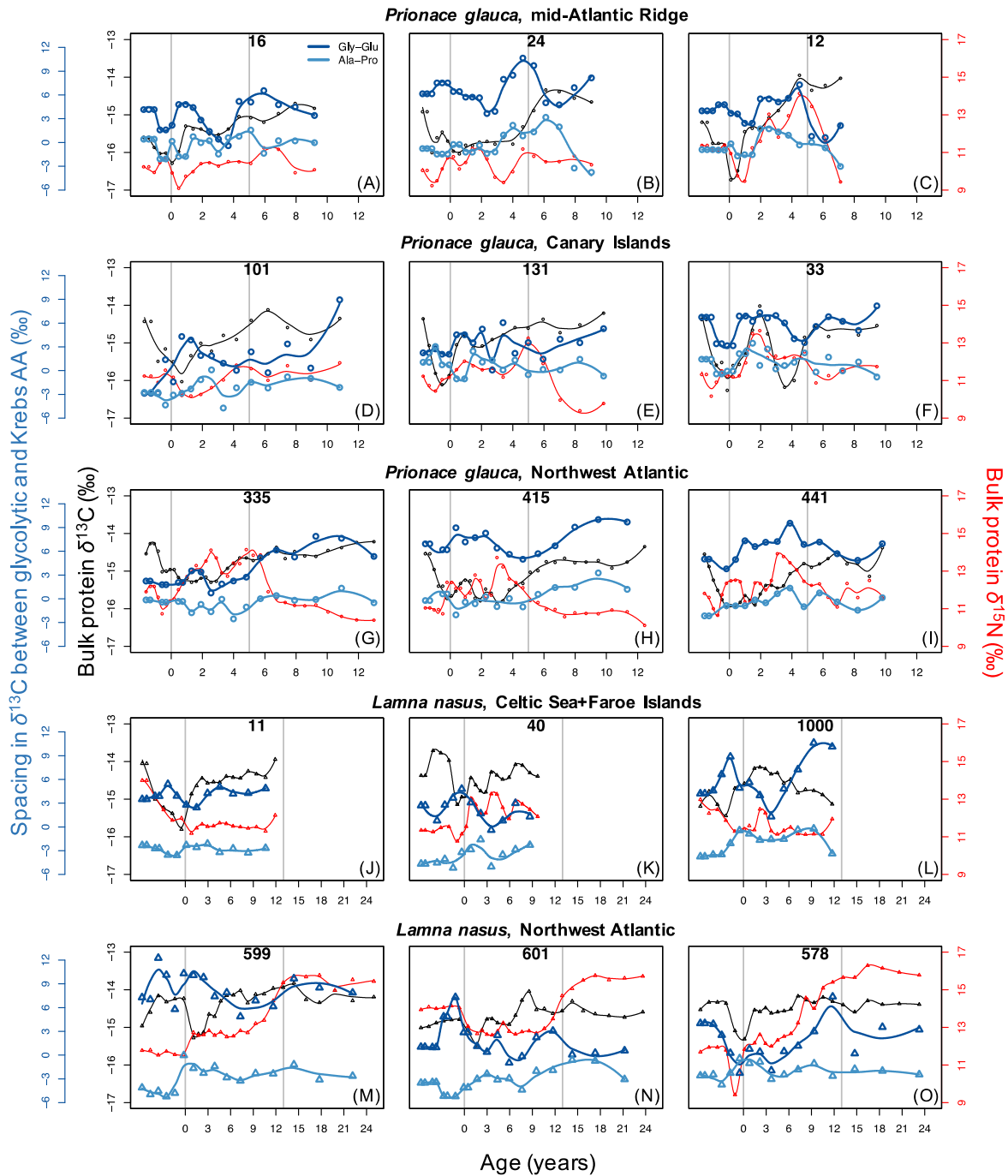


Figure S16. Individual profiles of spacing in $\delta^{13}\text{C}$ values between independent pairs of glycolytic (lipid-derived) and Krebs cycle (lipid+protein-derived) amino acids (glycine and glutamic acid, dark blue, and alanine and proline, light blue) and $\delta^{13}\text{C}$ (black) and $\delta^{15}\text{N}$ (red) values of bulk protein. Figure description is the same as for Fig. S4.

Tables

Table S1. Known $\delta^{13}\text{C}$ values of each amino acid in the reference materials AA1 and AA2 prior to derivatization measured at three laboratories (i.e., Woods Hole Oceanographic Institution, the Marine Biological Laboratory, and the UC Davis Stable Isotope Facility) and mean \pm SD values across laboratories.

Amino acid	WHOI	MBL	UC Davis	Mean \pm SD $\delta^{13}\text{C}$
Valine	-10.99	-10.55	-10.87	-10.80 \pm 0.23
Isoleucine	-10.82	-10.35	-10.69	-10.62 \pm 0.24
Leucine	-29.83	-30.00	-30.10	-29.97 \pm 0.14
Threonine	-10.62	-10.05	-10.65	-10.44 \pm 0.34
Phenylalanine	-11.46	-11.45	-11.54	-11.48 \pm 0.05
Alanine	-19.45	-19.15	-19.59	-19.40 \pm 0.23
Glycine	-37.86	-38.25	-38.26	-38.13 \pm 0.23
Proline	-10.79	-10.30	-10.67	-10.59 \pm 0.26
Aspartic acid	-22-17	-22.10	-20.96	-21.74 \pm 0.68
Glutamic acid	-28.24	-28.55	-28.52	-28.43 \pm 0.17

Table S2. Results for full generalized additive mixed effect models (GAMMs) predicting profile life history-normalized carbon and nitrogen isotopic compositions ($n\delta^{13}\text{C}$, $n\delta^{15}\text{N}$) of bulk protein in sequential vertebral samples from individual blue sharks and porbeagles caught across the North Atlantic. Estimated sample age was added as a smoother ($f(\text{Age})$), individual as random effect (random intercept) and species and capture area as parametric fixed effects ($f(\text{Species})$, $f(\text{Area})$; full model). Predictors with p-value <0.05 were considered significant (in bold).

Species	Parameter	$n\delta^{13}\text{C}$			$n\delta^{15}\text{N}$		
		DF	F	p-value	DF	F	p-value
All	$f(\text{Species})$	1	7.62	0.006	1	22.14	3.7510⁻⁶
	$f(\text{Area})$	4	0.75	0.56	4	4.55	0.001
	$f(\text{Age})$	7.75	26.46	<210⁻¹⁶	7.61	26.29	<210⁻¹⁶
	R^2 (adj.)	0.37			0.34		
	Scale est.	0.13			0.69		
	n	339			339		

Table S3. Degrees of freedom (DF) and Akaike Information Criteria (AIC) for GAMMs predicting profile life history-normalized carbon and nitrogen isotopic compositions ($n\delta^{13}\text{C}$, $n\delta^{15}\text{N}$) of bulk protein in sequential vertebral samples from individual blue sharks and porbeagles caught across the North Atlantic. The null model included estimated sample age as smoother and individual as random effect (random intercept) but no parametric fixed effects. Models with AIC lower than the null model were considered as optimal (in bold).

Species	Model	DF	$n\delta^{13}\text{C}$ AIC	$n\delta^{15}\text{N}$ AIC
All	d value = age+individual	5	319.95	882.85
	d value = age+individual+species	6	311.18	875.83
	d value = age+individual+species+area	10	316.15	865.93

Table S4. Mean \pm SD $\delta^{13}\text{C}$ values (‰) for individual amino acids in blue sharks and porbeagles.

Species	Essential amino acids				Non-essential amino acids				
	Valine	Isoleucine	Leucine	Phenylalanine	Alanine	Glycine	Proline	Aspartic acid	Glutamic acid
<i>P. glauca</i>	-21.25 \pm 2.20	-18.38 \pm 2.02	-26.52 \pm 2.22	-26.9 3 \pm 1.40	-13.69 \pm 1.81	-3.38 \pm 2.15	-13.50 \pm 1.43	-12.63 \pm 4.58	-8.11 \pm 1.87
<i>L. nasus</i>	-19.47 \pm 1.42	-17.83 \pm 2.01	-25.34 \pm 0.85	-25.66 \pm 0.73	-14.62 \pm 1.40	-0.95 \pm 2.18	-11.92 \pm 1.27	-13.24 \pm 4.59	-5.03 \pm 2.66